

# NUMERICAL SIMULATION OF A DUMMY FOR EVALUATION OF THERMAL ENVIRONMENT

**Fábio Alexandre Castelli, [fabiocastelli@gmail.com](mailto:fabiocastelli@gmail.com)**

**Anderson Morikasu Oshiro, [andmorioshiro@gmail.com](mailto:andmorioshiro@gmail.com)**

**Maurício Silva Ferreira, [mauserreira@gmail.com](mailto:mauserreira@gmail.com)**

**Guenther Carlos Krieger Filho, [guenther@usp.br](mailto:guenther@usp.br)**

Department of Mechanical Engineering, Polytechnic School, USP - Av. Prof. Mello Moraes, 2231, 05508-900, São Paulo, SP, Brazil

**Abstract.** *In this paper results from CFD simulation and experimental results from literature are compared to validate a geometry for numerical evaluation of thermal environment. A female dummy is discretized into 16 segments: head, chest, back, pelvis, arms, forearms, hands, thighs, legs and feet. For sensitivity analysis a simple geometry with cylindrical segments and a more complex geometry are used. The experiment was conducted with the dummy in a sitting position inside a wind tunnel with controlled conditions: fixed temperature and flow velocity from zero (stagnation condition) to 5m/s. The dummy has superficial temperature control for heat transfer analysis. In numerical simulation the Navier-Stokes equations and the radiative transfer equation are solved. A two-equations turbulence model is used, as well as the enhanced wall treatment that adapts both coarse and refined meshes in the boundary layer region. All the grid used in this paper are unstructured and composed by tetrahedral elements. There are layers of prismatic elements near the surfaces of the dummy to improve the heat transfer calculation. The grid for cylindrical geometry (here called the simple geometry) has approximately 3.8 million elements and the grid for complex geometry has approximately 4.6 million elements. The results show that the cylindrical geometry is sufficient to simulate the heat transfer by thermal convection and radiation. A more detailed geometry may not be advantageous due to the increased computational cost. The results also show that the adimensional  $y^+$  must be well controlled and the wall function must be well chosen.*

**Keywords:** *CFD, Heat transfer, Thermal manikin, Enclosed environment, Thermal comfort*

## 1. INTRODUCTION

University and industry are progressively developing analysis tools for thermal environment study. The principal application is to enhance the thermal comfort at indoor environments like airplane cabin, cars and inside buildings. The experimental approach could be avoided, despite its importance to validate numerical works. The numerical approach is more interesting because of its possibilities to operational cost reduction and time reduction to perform experiments.

In the literature, there are some studies evaluating heat transfer coefficients from experiments. [Nishi and Gagge \(1970\)](#) proposed a method based on mass and heat transfer analogy. The convective coefficient is obtained by sublimation rate of naphthalene balls fixed near the body surface. According to the author, the technique allows evaluate the convective heat transfer coefficient for dynamic activity like running and bicycle. [Ichihara et al. \(1995\)](#), [de Dear et al. \(1997\)](#) e [Yang et al. \(2009\)](#) used thermal manikin to estimate the heat transfer coefficients. In these researches, the correlation equation is valid for a range of air speed 0.05 to 1.4m/s (till 5m/s by [de Dear et al.](#) [Kurazumi et al. \(2008\)](#) tested the thermal manikins in various postures: stand, sitting, cross legs and supine. The intention was study the natural convection and the influence of surrounding temperature (varied from 26 to 16°C) on heat transfer.

This paper compares numerical results using commercial CFD code and experimental data from literature. The basic approach adopted in the experimental study by [de Dear et al.](#) involves a skin-temperature-controlled manikin exposed to a variety of air speed in a wind tunnel. The virtual manikin is divided into 16 parts: head, chest, back, pelvis region, arms, forearms, hands, thighs, legs and feet. Natural and forced convection and radiation heat transfer coefficient are evaluated for a range of air speed 0.05 to 5 m/s.

The main objective of the present article is validating a computational manikin by analyzing geometrical influence.

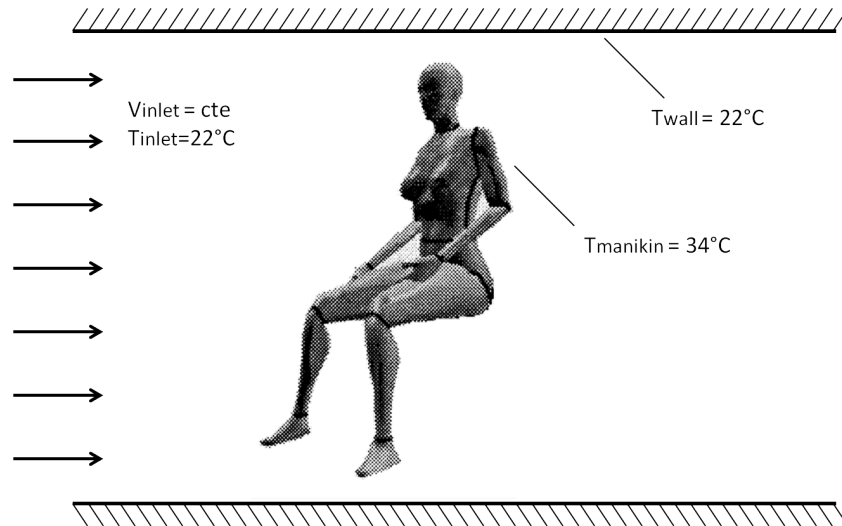


Figure 1. Experimental apparatus

This study is a first step necessary to prepare subsequent researches in thermal environment analyze and application in thermal comfort.

## 2. EXPERIMENTAL SETUP

The experiments in [de Dear \*et al.\* \(1997\)](#) were conducted in the wind tunnel located in the Centre for Environmental Design Research, University of California at Berkley. This wind tunnel is approximately 16m long from air intake to work section. The manikin used for these experiments resembles a female dummy, which has 16 independent body segments, 1.5m tall and  $1.471m^2$  of surface area. The Fig.1 shows a schematic representation of the experimental apparatus and the virtual manikins.

To allow temperature control the dummy is covered with thermocouples. The rate of heat loss was estimated with the electrical power required to maintain the temperature at a constant value.

The supplied air temperature and temperature of wind tunnel's wall were maintaining constant at 22°C. The whole manikin surface temperature was set at 34°C. Eight inlet velocities in wind tunnel were used: 0.05m/s for evaluate natural convection and 0.2, 0.5, 0.8, 1.2, 2.0, 3.0 and 5.0m/s for forced convection. The paper also investigates eight wind directions – 0° (facing into the wind), 45°, 90° (right-side), 135°, 180° (back to the wind), 225°, 270° (left-side) and 315°, starting with 0° (facing into the wind) to 315°, for evaluate the effects of wind direction.

## 3. MATHEMATICAL AND NUMERICAL MODELING

The turbulent flow around the manekin is simulated using the commercial CFD code Ansys Fluent®, based on the finite volume method. To account for the turbulent flow, RANS based turbulence modelling is used. A transport equation for a general quantity  $\psi$  can be written as shown in Eq.1.

$$\frac{\partial \bar{\rho} \tilde{\psi}}{\partial t} + \frac{\partial \bar{\rho} \tilde{\psi} \tilde{u}_j}{\partial x_j} = \frac{\partial}{\partial x_j} (\Gamma_\psi \frac{\partial \tilde{\psi}}{\partial x_j}) + S_\psi, \quad (1)$$

$\tilde{\psi}$  is the density-weighted averaging of the general quantity,  $\bar{\rho}$  is the time averaged density of the air,  $t$  is the time,  $x_j$  is the spatial cartesian coordinate in  $j$  direction,  $\tilde{u}_j$  is the density-weighted averaging of the Cartesian component of velocity in  $j$  direction,  $\Gamma_\psi$  is the diffusivity of the transported quantity and  $S_\psi$  can be used to account for source terms of the equation.

The quantities transported in simulations are momentum, turbulent kinetic energy, turbulent kinetic energy dissipation,

enthalpy and mass.

In Ansys Fluent® the pressure based approach is used to do the coupling between pressure and velocity. To account for the thermal plume formed above the dummy the air gas is modeled by the Boussinesq Model that considers the density fluctuation only in buoyancy term of the moment equation. Using the Boussinesq approximation the buoyancy term in the momentum equation reads  $(\rho - \rho_o)g \approx -\rho_o\beta(T - T_o)g$ , where  $\rho_o$  is the reference density of the flow,  $T_o$  is the operating temperature, and  $\beta$  is the thermal expansion coefficient.

Since a pressure based approach is adopted, a velocity-pressure coupling method is necessary. The SIMPLE (Semi-Implicit Method for Pressure-Linked Equations) is adopted (Versteeg and Malalasekera (2007)).

The K-epsilon RNG Model is used to account for the turbulence effects. The option for this model was done because the satisfactory accuracy and low computational cost in problems involving flow indoors (Zhai *et al.* (2007) and Zhang *et al.* (2007)). The standard values of the model parameters are used in the simulations done in this work.

The discretization of the advective terms (second term in Eq.1) of transport equations is done with the second order Upwind Scheme. Nevertheless, the discretization of the diffusive terms (third term in Eq.1) was done with the Central Difference Scheme (CDS).

The influence of radiation on the heat transfer is accounted for with the discrete ordinate model. The radiative transfer equation in the direction  $\vec{s}$  is presented by Eq.2. For a given direction this equation is treated numerically in the same manner as Navier-Stokes and other transport equations as Eq.1 (Fluent Inc. (2006)).

$$\nabla \cdot (I(\vec{r}, \vec{s})\vec{s}) + (a + \sigma_s)I(\vec{r}, \vec{s}) = a \frac{\sigma T^4}{\pi} + \frac{\sigma_s}{4\pi} \int_0^{4\pi} I(\vec{r}, \vec{s}') \Phi(\vec{s}, \vec{s}') d\Omega' \quad (2)$$

$I$  is the radiative intensity,  $\vec{r}$  is the position vector and  $\vec{s}$  is the direction of the ray path. Considering the walls as diffuse reflecting surfaces, the boundary conditions for Eq.2 is represented by Eq.3. In this work the non-participating medium model is used. In order to do that, the scattering factor  $\sigma_s$  and the absorption coefficient  $a$  are set to zero. Walls are assumed to be gray bodies with emissivity  $\epsilon=0.9$ . The body intensity is given by the Planck distribution and is evaluated at wall temperature (Modest (2003)).

$$I(\vec{r}_w, \vec{s}) = \epsilon(\vec{r}_w)I_b(\vec{r}_w) + [1 - \epsilon(\vec{r}_w)]/\pi \int_{\vec{n} \cdot \vec{s} < 0} I(\vec{r}_w, \vec{s}') |\vec{n} \cdot \vec{s}'| d\Omega' \quad (3)$$

$\vec{r}_w$  is the position vector at wall and  $d\Omega$  is the discrete solid angle. The direction domain was discretized with 2x2 solid angles in the polar and azimuthal spherical coordinates.

#### 4. CFD PRE-PROCESSING

A plausible definition of the boundary conditions is highly important. The air flow entering the domain received a velocity inlet boundary treatment. This approach prescribes a constant air velocity and allows total pressure to vary in function of the inner solution. The inflow direction was set normal to the boundary. Information on the turbulence is also required for complete boundary conditions definition. The air inlet turbulence intensity was set from 4.1 to 8.4% depending on the input air speed, in agreement with the experiment (de Dear *et al.* (1997)). The length scale was set to 0.5 m according to the dummy's body size.

Flow outlet exiting the wind tunnel was treated with outflow condition. This boundary condition is adequate when the details of the flow velocity and pressure are not known prior to solution of the problem (Fluent User Guide). The solution is extrapolated from the flow field.

Both virtual manikins is developed based on dimension of manikin "Monika" used in the experimental study. The simple manikin was created using Solid Works® and the detailed manikin was imported from Ramsis®. Figure below shows the manikins.

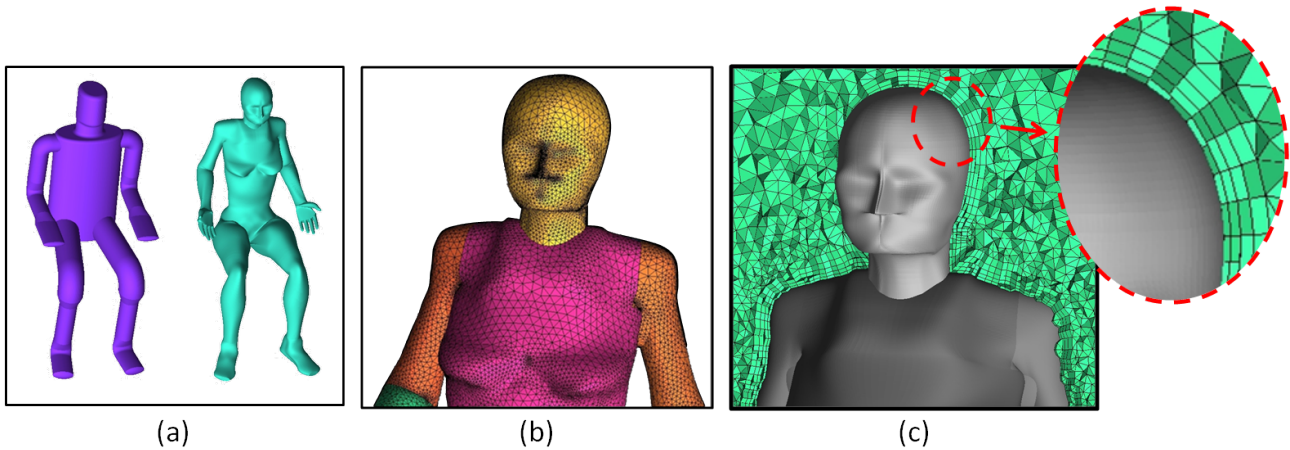


Figure 2. Geometry of simple and complex manikins (a), superficial grid on complex geometry (b) and volumetric grid on complex geometry (c).

For this work a computational grid with 3.8 million elements was generated for simple geometry and a computational grid with 4.6 million was generated for complex geometry. The Fig.3 shows the superficial and the volumetric grid for complex geometry. These grids are unstructured and composed by tetrahedral elements. Better refinements are employed in the near dummy's skin region. To enable best results a prism layer with four elements along 15mm is applied around the manikin surface.

## 5. RESULTS

The Fig.3 shows the velocity contours and the velocity vectors in a transverse plane cutting the manikins. The results for lower air velocities predicts the thermal plume around the dummy and the recirculation zone in front of the dummy, as expected. For higher speeds, the displacement of the boundary layer on the back causing a recirculation zone in the region downstream of the flow.

The Tab.1 shows the natural convection coefficient and thermal radiation coefficient obtained in experiments of de Dear *et al.* (1997) and from numerical simulations for wind speeds below 0.1m/s. These coefficients were calculated by dividing the heat loss of each segment by the temperature difference between of skin and the reference value equal to 22°C.

Table 1. Thermal radiation transfer coefficients  $h_r$  and natural convection coefficient  $h_c$  for air speeds below 0,1m/s. (\*) experimental coefficients.

Segment	$h_r (Wm^{-2}K^{-1})$			$h_c (Wm^{-2}K^{-1})$		
	de Dear*	CFD complex	CFD simple	de Dear*	CFD complex	CFD simple
foot (left and right)	4,2	5,61	6,49	4,2	3,93	2,63
lower leg (left and right)	5,4	5,31	6,70	4,0	3,62	2,37
thigh (left and right)	4,6	4,78	5,63	3,7	3,29	2,00
pelvis	4,8	4,82	5,98	2,8	2,92	1,08
head	3,9	5,48	6,31	3,7	3,03	2,01
hand (left and right)	3,9	4,43	5,11	4,5	6,45	2,59
forearm (left and right)	5,2	4,75	5,11	3,8	3,95	2,24
upperarm (left and right)	4,8	5,08	5,92	3,4	3,54	2,41
chest	3,4	5,03	5,73	3,0	3,13	2,09
back	4,6	5,04	6,14	2,6	2,43	1,15
whole body	4,5	5,04	5,93	3,3	3,47	2,01

For whole body the simple manikin simulation underestimates the natural convection coefficient in about 40% while

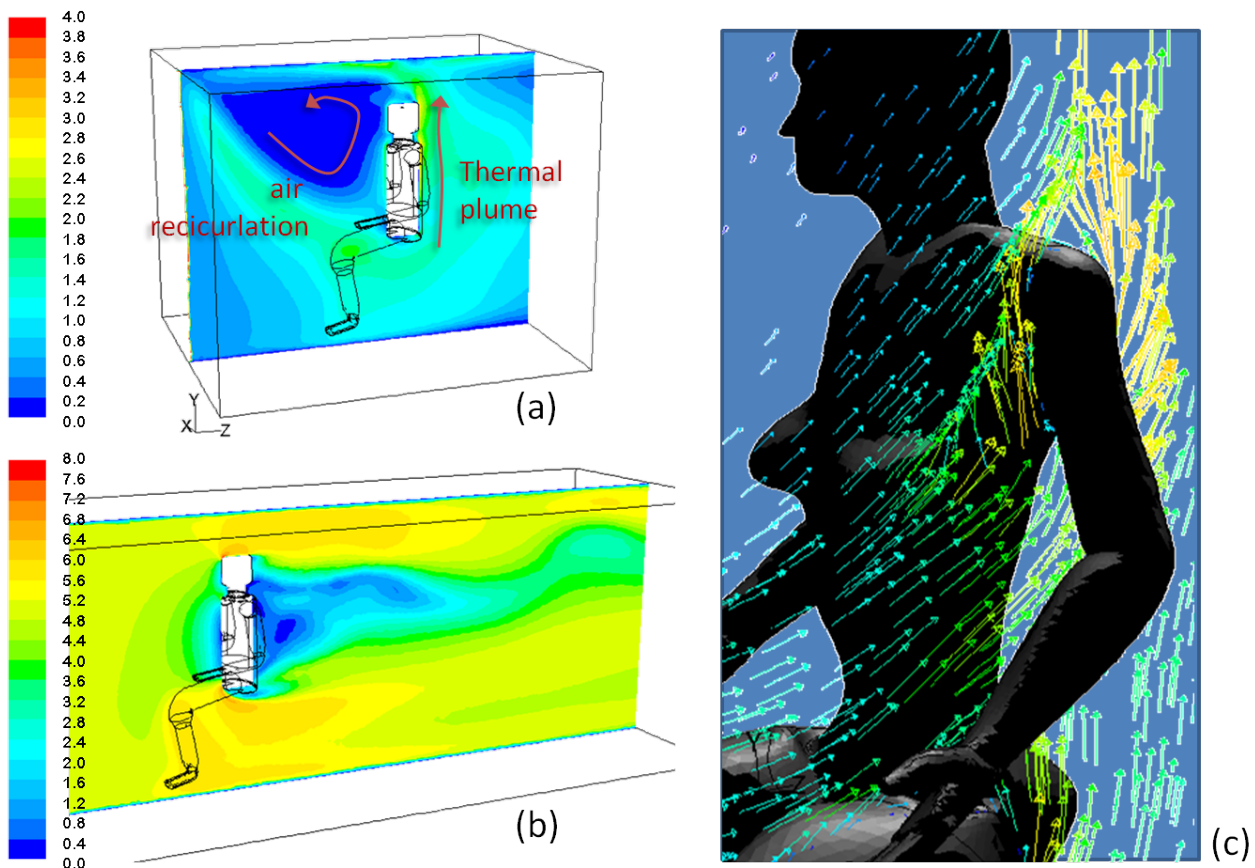


Figure 3. Contours of velocity at transversal plane cutting the simple manikin for 0.05m/s air speed (a), for 5m/s air speed (b) and vector of velocity at transversal plane cutting the complex geometry for 0.05m/s air speed (c).

the complex manikin simulation overestimates this coefficient in about 5%. The results for the complex manikin differ more in the hands, coincidentally where the level of geometric detail is greater (smaller radius).

Both numerical results underestimate thermal radiation. The complex manikin simulation overestimates about 12% while the simplified manikin simulation overestimates about 30%.

The Figs.4 and 5 summarize the numerical and experimental thermal convection results as a function of air velocity. The experimental results are described by the regression curves representing the mean value for eight azimuthal directions of air flow. The experimental values range about 15 and 30% around the regression curve.

The numerical results of thermal convection overestimate the experiments, probably because unequal spatial distribution of the segments or numerical error due to the limitation of the wall model treatment, especially for more complex manikins. As Fig6, in areas with smaller radius, as fingertips, the rate of heat loss amount is greater. Under the same regions the dimensionless  $y^+$  is greater. Furthermore, for air velocity of 5m/s, the decrease in heat loss along the back of the manikin suggests that the numerical model anticipates the boundary layer detachment.

Considering mean values for whole body and flow velocities until 0.8m/s the complex manikin simulations overestimate about 15% the thermal convection coefficient while the simple dummy simulations overestimate about 30% this coefficient, but the actual error is smaller since the experimental coefficients described by regression curves represents an average for eight azimuthal directions of air flow.

## 6. DISCUSSION

As well as in experimental work of *de Dear et al. (1997)*, in present numerical approach, eight conditions are simulated: inlet velocity of 0.05m/s for natural convection and 0.2, 0.5, 1.2, 2.0, 3.0 and 5.0m/s to forced convection. Are used the

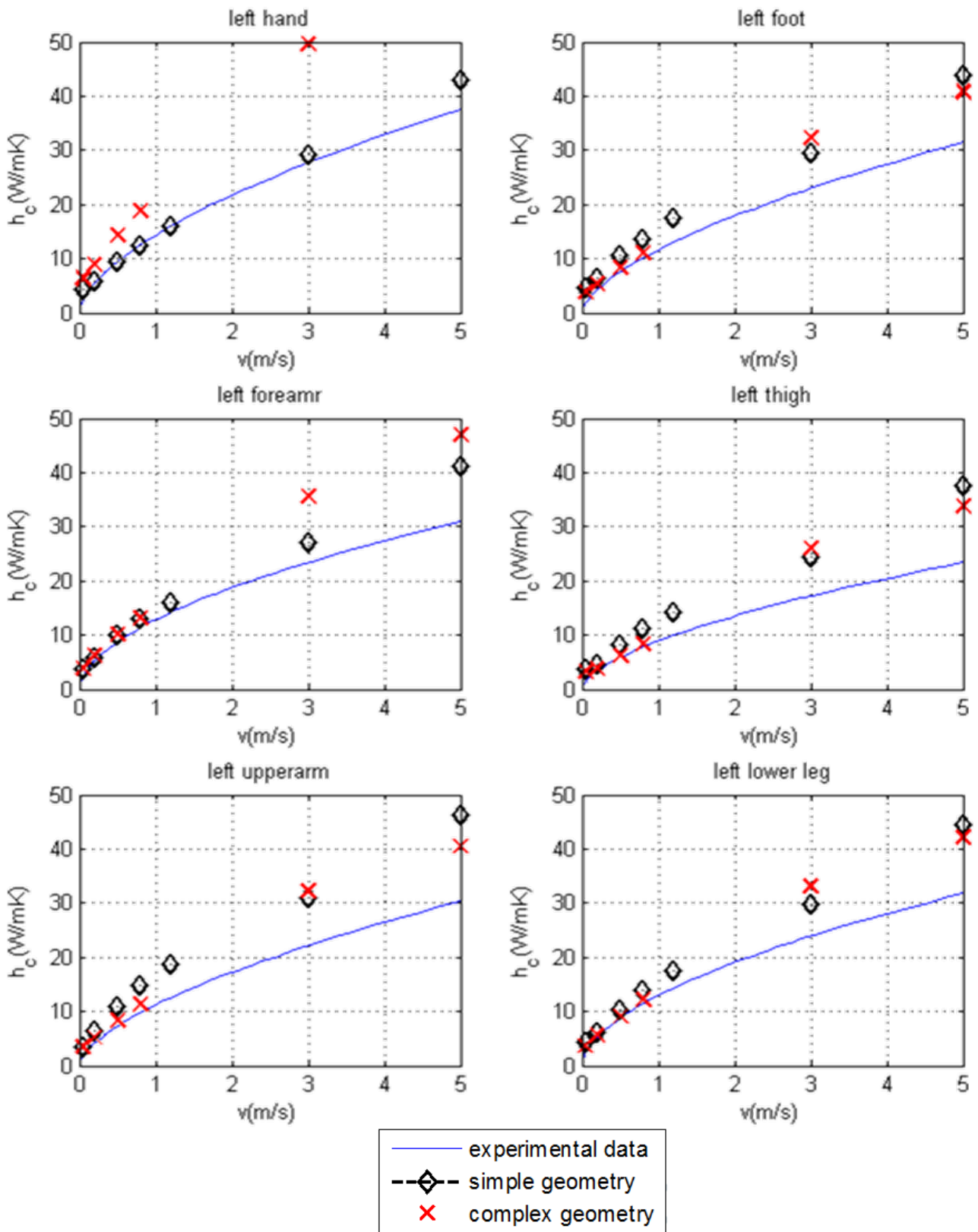


Figure 4. convection coefficients results: upper and lower limbs.

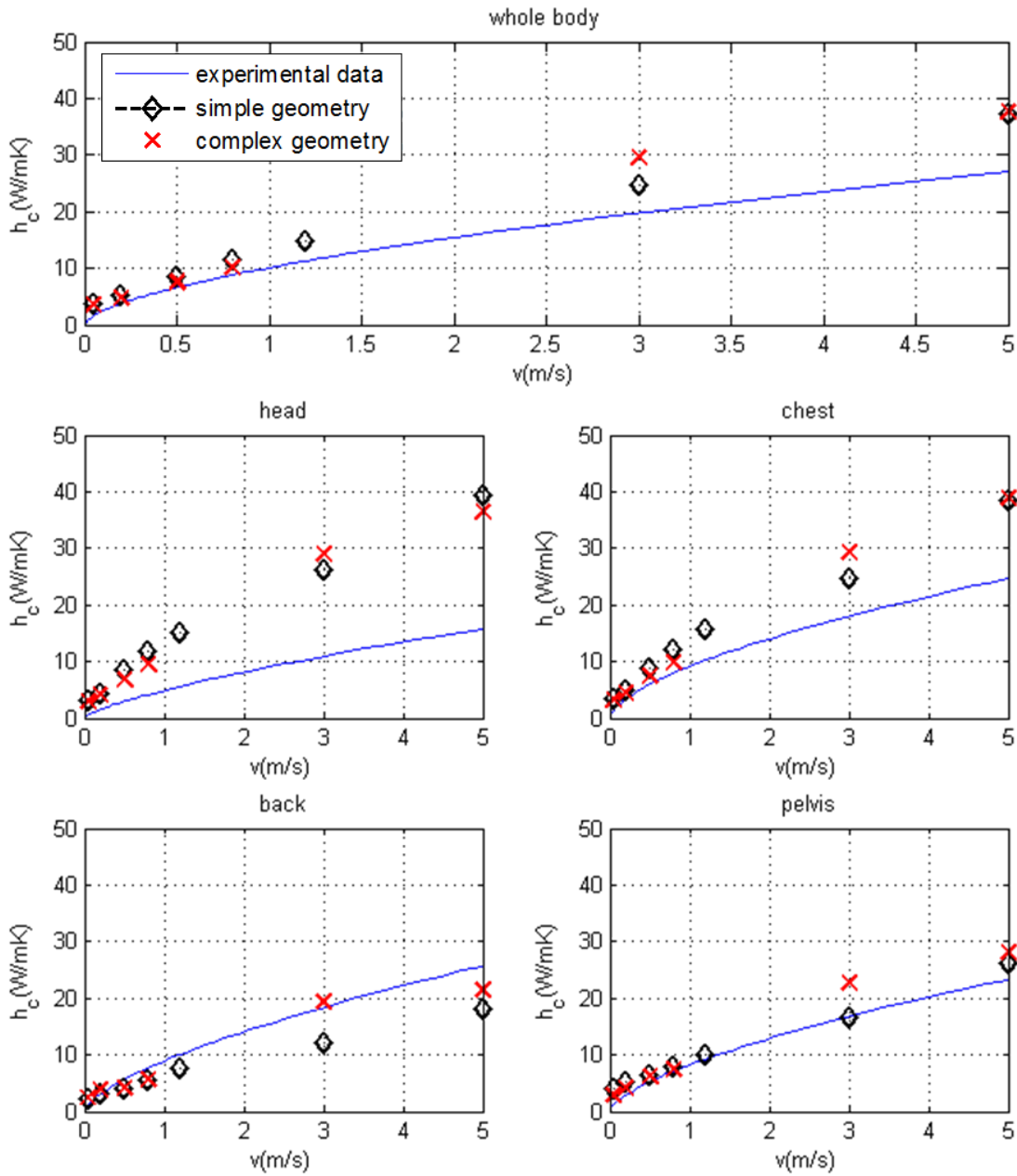


Figure 5. convection coefficients results: head, chest, back pelvis and results for whole body.

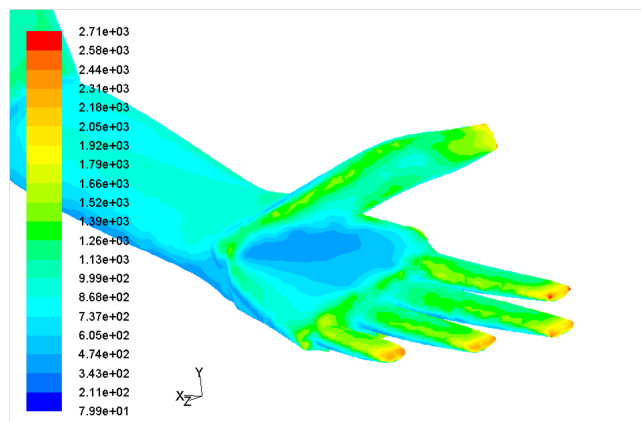


Figure 6. Contours of total heat flux on hand ( $\text{w/m}^2$ ).

enhanced wall treatment, the Discrete Ordinates radiation model and Boussinesq model to account for buoyancy.

The qualitative results as air flow distribution, recirculation zones and thermal plume were diagnosed as intended. The performance of the Boussinesq model to accounting for the buoyancy is satisfactory.

The heat exchange results along the numerical manikins show deviations from the experimental values. The level of geometry detail and spatial arrangement of body segments and walls surrounding influence the thermal radiation calculation. Are expected radiation results between 10 and 30% higher than the experimental values.

The thermal convection results depend on the performance of the wall treatment model. Simulations of situations that differ from flow in flat plate tend to overestimate the thermal convection. At the speeds until 0.8m/s are expected errors lower than 15% for more accurate geometries and lower than 30% for simplified geometry.

## 7. REFERENCES

- de Dear, R.J., Arens, E., Hui, Z. and Oguro, M., 1997. "Convective and radiative heat transfer coefficients for individual human body segments". *International Journal of Biometeorology*, Vol. 40, pp. 141–156.
- Fluent Inc., 2006. *FLUENT 6.3 User's Guide*.
- Ichihara, M., Saitou, M., Tanabe, S. and Nishimura, M., 1995. "Measurement of convective heat transfer coefficient and radiative heat transfer coefficient of standing human body by using thermal manikin". *Proceedings of the annual meeting of the architectural institute of Japan*, pp. 379–380.
- Kurazumi, Y., Tsuchikawa, T., Ishii, J., Fukagawa, K., Yamato, Y. and Matsubara, N., 2008. "Radiative and convective heat transfer coefficients of the human body in natural convection". *Building and environment*, Vol. 43, pp. 2142–2153.
- Modest, M.F., 2003. *Radiative Heat Transfer*. Academic Press.
- Nishi, Y. and Gagge, A.P., 1970. "Direct evaluation of convective heat transfer coefficient by naphthalene sublimation". *Journal of applied physiology*, Vol. 29, pp. 830–838.
- Versteeg, H.K. and Malalasekera, W., 2007. *Computational Fluid Dynamics - The Finite Volume Method*. Pearson, second edition edition.
- Yang, J., Kato, S. and Seo, J., 2009. "Evaluation of the convective heat transfer coefficient of the human body using the wind tunnel and thermal manikin". *Journal of asian architecture and building engineering*, Vol. 8, pp. 563–569.
- Zhai, Z., Zhang, Z., Zhang, W. and Chen, Q., 2007. "Evaluation of various turbulence models in prediction airflow and turbulence in enclosed environments by cfd: Part 1 - summary of prevalent turbulence models". *HVACR Research*, Vol. 13, No. 6.
- Zhang, Z., Zhang, W., Zhai, Z. and Chen, Q., 2007. "Evaluation of various turbulence models in prediction airflow and turbulence in enclosed environments by cfd: Part 2 - comparison with experimental data from literature". *HVACR Research*, Vol. 13, No. 6.